January 2014

Electrical Impedance Myography And Quantitative Ultrasound As Biomarkers In Duchenne Muscular Dystrophy

Irina Shklyar

Electrical Impedance Myography and Quantitative Ultrasound as Biomarkers in Duchenne Muscular Dystrophy

A Thesis Submitted to the

Yale University School of Medicine

in Partial Fulfillment of the Requirements for the

Degree of Doctor of Medicine

by

Irina Shklyar

2014

ELECTRICAL IMPEDANCE MYOGRAPHY AND QUANTITATIVE ULTRASOUND AS BIOMARKERS IN DUCHENNE MUSCULAR DYSTROPHY

Irina Shklyar and Seward B. Rutkove. Department of Neurology, Beth Israel Deaconess Medical Center, Boston, MA. (Sponsored by Jonathan M. Goldstein, Department of Neurology, Hospital for Special Surgery, New York, NY).

Electrical impedance myography (EIM) and quantitative ultrasound (QUS) represent two rapid, non-invasive, quantitative, and child-friendly approaches to measure disease outcomes in clinical trials that may surpass functional tests currently in use. In this thesis, we present a comparison of EIM and QUS data in six muscles from 25 DMD and 25 healthy subjects, aged 2-14 years. Quantitative ultrasound data can be analyzed by measuring the brightness, or grayscale level (GSL), of the ultrasound image. To circumvent post-processing variability across manufacturers, for the first time, we introduce a new means of evaluating QUS—a quantitative backscatter analysis (QBA) on the raw radio frequency (RF) signal received by the ultrasound probe in DMD and control subjects. For EIM, either the phase at 50 kHz or the phase ratio (50 kHz/200 kHz) was used for measuring disease status. We found that taking the phase ratio substantially reduces the confounding effect of subcutaneous fat thickness on EIM ($r=0.16$, $p=0.45$) compared with the standard phase at 50 kHz ($r=-0.72$, $p<0.0001$) in averaged muscles. Using age as a surrogate for disease severity, we found that 50 kHz phase decreased with age in select muscles while GSL did not. The averaged phase correlated strongly with the North Star Ambulatory Assessment (NSAA) ($rho=0.735$, $p=0.004$), while GSL did not ($rho=-0.442$, $p=0.115$). Although the standard phase at 50 kHz averaged values did not correlate with GSL, the phase ratio did ($rho=-0.48$, $p=0.017$). In DMD, age showed comparable correlation with “superficial” region of interest (ROI) QBA and GSL (average: $rho=0.67$, $p=0.0004$ vs. $rho=0.47$, $p=0.020$), in contrast to “whole muscle” ROI, and the difference in rho values did not reach significance (average: $z=1.00$, $p=0.16$). Here, we show that “whole muscle” GSL detects disease pathology from an early age and remains stable over time; in contrast, DMD and control subjects begin with relatively similar EIM values and diverge with age. The moderate correlation between averaged EIM and QUS parameters indicate that the measures provide both overlapping and divergent information about dystrophic muscle. Our data confirm that EIM and QUS show promise as outcome measures that may aid the rapid identification of successful therapeutics currently in clinical pipelines.

I would like to acknowledge my family and Mark Scott, to whom I am forever indebted. I would like to express my sincere gratitude to my research supervisor Dr. Seward Rutkove and my thesis advisor Dr. Jonathan Goldstein.

Contents

1. INTRODUCTION

1.1 Duchenne muscular dystrophy

Duchenne muscular dystrophy (DMD), caused by mutations in the dystrophin gene, is the most common childhood neuromuscular disease—the disease affects one in every 3,500 live male births [1]. The disease is characterized by progressive muscle wasting, leading to disability followed by early death by age 30. To date, corticosteroids are the only known treatment; however, these medications only mildly slow disease progression [2].

While several promising therapies for DMD are undergoing clinical trials, there remains an urgent need for more sensitive biomarkers for disease progression to rapidly and reliably identify successful candidate therapies.

1.2 Outcome measures in Duchenne muscular dystrophy clinical trials

Outcome measures for DMD clinical trials remain limited to functional measures such as the six-minute walk test [3] and North Star Ambulatory Assessment (NSAA) [4]. While useful, functional measures are constrained by subjective elements such as effort and mood, as well as high variability in young boys and ineffectiveness in non-ambulatory boys [5, 6]. The development of

new DMD therapeutics will therefore require sensitive, reliable, and affordable objective tests, in addition to functional tests, that can detect subtle changes in disease status, as well as ones that are applicable to all DMD patients with variable degrees of disability. Computerized tomography, magnetic resonance imaging, dual x-ray absorptiometry, and serologic tests have been employed in the evaluation of patients with neuromuscular diseases, but these are limited by inadequate specificity or excessive time, cost, radiation exposure, or invasiveness [7, 8].

1.3 Quantitative ultrasound

Ultrasound (US) shows increased echointensity in the muscles of DMD subjects, due to adipose and connective tissue deposition, compared with healthy muscle [9, 10]. US is typically only employed as a qualitative imaging modality. However, the brightness of muscle can be quantified (quantitative ultrasound, QUS) by measuring grayscale level (GSL) using image processing software; this provides a means of comparison between diseased and healthy muscle. Rutkove and others have used this approach and have shown that it sensitive to changes in spinal muscular atrophy and DMD [11, 12].

Ultrasound images are generated by measurement of the acoustic energy scattered back from the image, known as backscatter. This information is compressed using proprietary algorithms into 256 GSLs for image display. The distribution of the backscattered energy received by the ultrasound probe may not be uniformly displayed across the dark to bright GSL spectrum and can vary between systems and settings. The backscattered energy level can be estimated from GSLs by determining the compression curve and by reference to an external phantom.

Rather than evaluating a post-processed image, quantitative backscatter analysis (QBA), an alternate form of QUS, evaluates the raw radio frequency (RF) backscattered acoustical data. This approach is appealing because there are no hidden transformations of the data before analysis [12, 13]; this can potentially increase repeatability across multiple visits and various ultrasound manufacturers.

Here, for the first time, we use actual backscatter values rather than estimated backscatter using a calibrated phantom [14], a potentially cumbersome process. It is unknown if measurement of the backscattered energy levels, as opposed to GSLs, better detects and quantifies pathology. Furthermore, it is unknown whether post-processing of backscatter results in skewed data that does not accurately reflect muscle properties.

1.4 Electrical impedance myography

Electrical impedance myography (EIM), which uses localized impedance measurements of muscle, is a non-invasive, painless method that can potentially quantify disease status and change in disease over time in DMD. EIM values have been shown to be sensitive to the severity of other neuromuscular diseases and useful biomarkers of disease progression in amyotrophic lateral sclerosis (ALS) and in spinal muscular atrophy (SMA) [15-25]. Although prior work has emphasized single-frequency data, here we explore the ratio of data at two frequencies as a means of recognizing spurious data and identifying new outcome measures of disease. The properties that EIM is detecting are still being investigated, although it is believed to measure loss of muscle tissue and deposition of connective tissue. Quantitative ultrasound may provide a clue to the aspects of disease that EIM is measuring if the acoustic QUS data and electric EIM data demonstrate overlap. Both techniques are child-friendly, require no patient effort, are rapid to test, and can measure numerous muscles. Therefore, we are assessing the value of both EIM and QUS as potential biomarkers for DMD clinical therapeutic trials.

1.5 Objectives

The objective of this cross-sectional analysis of DMD and control subjects is to determine how well EIM and QUS parameters identify disease status, how they correlate with age and NSAA as surrogates of disease severity, and how the two measures correlate with one another in order to identify how much EIM data relates to QUS data. We hypothesize that both EIM and QUS can help identify the presence of disease and correlate with other markers of disease severity; furthermore, we hypothesize that EIM will correlate to QUS to some extent due to detection of similar pathologic features of dystrophic muscle. However, we do not expect full overlap because of the divergent aspects of the acquired acoustic and electrical data.

In this study, we also performed and compared measures of backscatter and GSL from ultrasound images of muscle obtained from healthy boys and those with DMD and compared results to age and the NSAA as surrogates of disease severity.

2. SPECIFIC AIMS

Hypothesis. EIM and QUS parameters can serve as accurate measures of disease status and progression in Duchenne Muscular Dystrophy (DMD) that may surpass the functional measures currently in use. We will assess this hypothesis via the following aims:

Specific Aim #1: To identify whether the North Star Ambulatory Assessment is closely associated with EIM and QUS parameters via a cross-sectional analysis. Rationale: As an assessment of a new biomarker's validity, it must correlate with established functional tests. Using data from one visit for all DMD boys, cross-sectional analyses will be performed to determine the relationship between the EIM and QUS data and the North Star Ambulatory Assessment (NSAA), aiming to identify those measures which are most closely aligned to the EIM and QUS results in the DMD boys. This will be completed via standard Spearman correlations.

Specific Aim #2: To evaluate how EIM and QUS parameters change with age in a group of DMD boys as compared to normal subjects as a surrogate of disease progression. Rationale: In a cross-sectional analysis, age can be used as a surrogate for the passage of time and degree of decline. We aim to make comparisons to the data obtained in the DMD and healthy subjects

to determine how effective QUS and EIM parameters are at detecting disease severity.

Specific Aim #3: To assess the test-retest repeatability of QBA and GSL in a group of boys with DMD and in a group of age-matched healthy controls as well as the intra- and inter-examiner reliability of EIM and QUS parameters. Rationale: For any biomarker to be useful, it must show excellent repeatability. Standard tests of repeatability, including percent variation, intra-class correlation analysis, and Bland-Altman analysis will be performed to compare EIM and QUS data.

3. METHODS

3.1 Subjects and recruitment

The institutional review board of Children's Hospital Boston approved the protocol. Informed written consent and verbal assent were obtained, respectively, from, parents and children. All subjects were male and age 2 years to 14 years. Subjects were not permitted to have a pacemaker or other electrical device for inclusion in the study. All subjects with DMD had genetic confirmation of disease. DMD subjects were excluded if they were involved in an ongoing clinical trial (outside of a natural history study) or if they had another neuromuscular or other medical condition that substantially impacted health. They were recruited through the Neurology Clinic at Children's Hospital Boston. Healthy subjects did not have a history of neuromuscular disease or other disease that would substantially impact health. They were recruited by advertisement and via family members. This research is part of a larger longitudinal study; as a result, the earliest visit for which as much data as possible was available was used for each subject.

3.2 EIM measurements

EIM measurements were obtained with the Imp SFB7 (Impedimed, Inc, Sydney Australia), using a custom hand-held array previously described [25]. Three probe sizes were used to account for child size. Unilateral measurements were performed on the dominant extremities on deltoid, biceps, wrist flexors, quadriceps, tibialis anterior, and medial gastrocnemius muscles. Although all EIM measurements were done longitudinally and transversely—parallel and orthogonal to muscle fibers, respectively—only transverse measurements were analyzed here. This was done because prior work in the mouse model of DMD, known as mdx, demonstrated that transverse data showed greater differences than parallel data [26]. Additionally, the US measurements were performed transversely, so the use of transverse EIM and US data ensured that identical regions were evaluated. Anatomical placement of EIM and US probes is described in Table 1.

Table 1: Locations of Ultrasound Measurements

Muscle	Location
Deltoids	One-fifth distance from acromion to lateral epicondyle
Biceps Brachii	Arm supine, two-thirds distance from acromion to antecubital fossa
Wrist/Finger Flexors	Arm supine, one-third distance from the medial epicondyle to base of thumb
Quadriceps	Two-thirds distance from inguinal crease to superior aspect of patella, seated knee bent
Tibialis Anterior	One-fourth distance from fibula head to lateral malleolus midpoint, seated, ankle neutral
Medial Gastrocnemius	One-third distance from inferior aspect of popliteal fossa to medial malleolus, seated, ankle neutral

EIM measures voltage while a small current is being applied. Diseased muscle has larger voltage and decreased phase shift. The SFB7 collects information on the resistance (R) and reactance (X) at different frequencies, and the phase is obtained from calculating arctan (X/R). The phase is then plotted against frequency. We used the phase at 50 kHz in standard use for this analysis, as well as the ratio of phase at 50 kHz to phase at 200 kHz. This ratio was optimized to diminish the impact of SF thickness. Figure 1 demonstrates the EIM probe used

as well as sample phase graphs of a DMD and control subject at different frequencies.

For EIM reliability, biceps and quadriceps measurements were obtained by two examiners for a set of baseline visits, and one examiner repeated measurements within the session. Additional measurements on all muscles were obtained 3-7 later to determine inter-session reliability.

3.3 Ultrasound measurements

US images were obtained using the Terason t3000 system (Teracorp, Inc, Burlington, MA) with a 10 MHz probe. Measurements were performed on the same muscles and locations as the EIM measurements, and the probe was placed transversely. Still images were acquired, and US settings were kept constant for all image acquisition. All images were analyzed using image processing software to obtain the brightness of the region of interest, measured as median grayscale level (GSL), as shown in Figure 1.

The superficial region of interest (ROI) was defined as the 250 pixel by 50 pixel rectangle (1 cm x 0.5 cm) within muscle immediately below the layer of subcutaneous tissue and above bone. These ROI dimensions were selected to fit within the muscles of the youngest subjects recruited. This was used for the analysis of QBA and GSL to ensure that like regions were compared. The ROI

size was decreased to fit within the fascia surrounding the rectus femoris to avoid artifact from intermuscular fascia. The whole muscle ROI was defined as the entire depth of muscle below the subcutaneous fat layer and above bone, excluding 25 pixels of the lateral margins to avoid artifact. This was used to ensure the area assessed by EIM was similar in size compared to GSL.

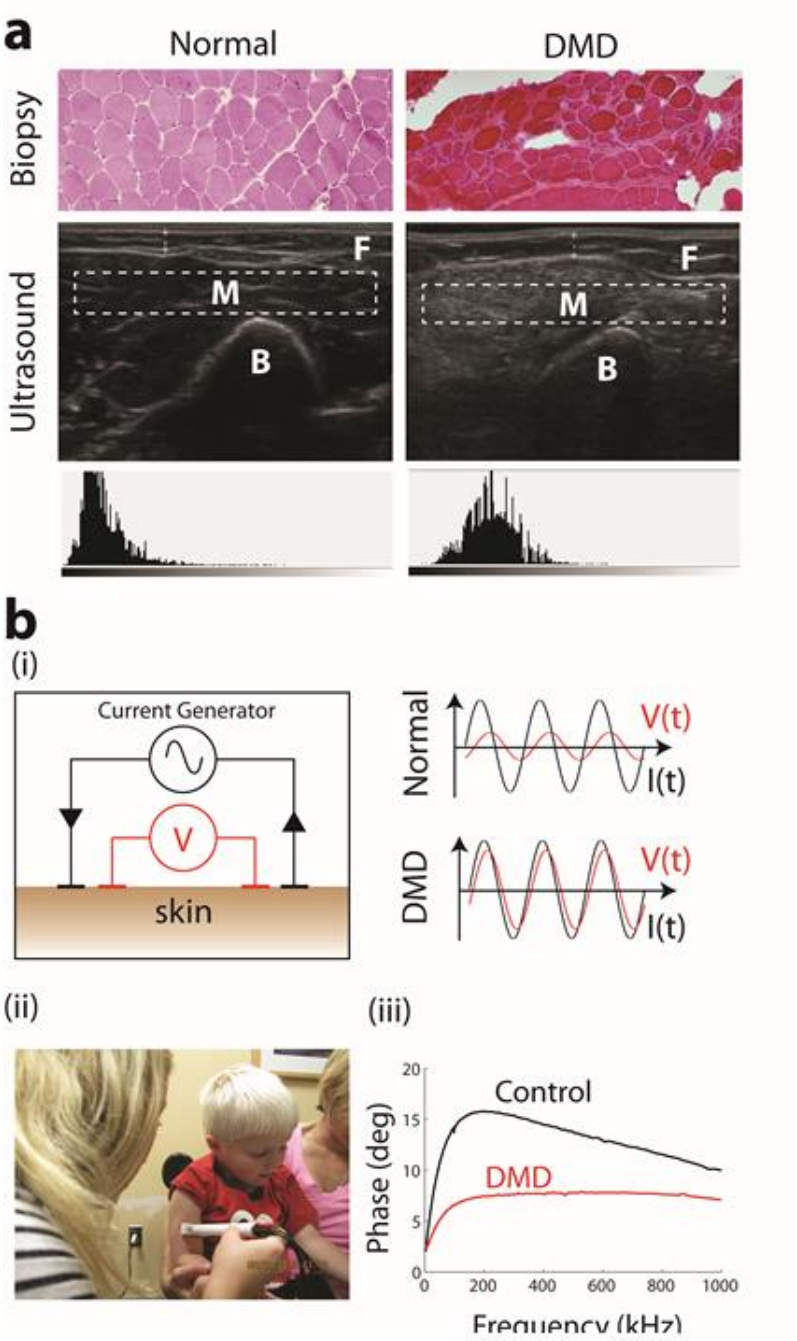

Figure 1. Quantitative Ultrasound (QUS) and Electrical Impedance Myography (EIM). a. Muscle biopsies and US images of biceps muscles in control and DMD subjects, 11-years-old. This is an example of increased echogenicity in the muscle of a DMD subject compared with control. Histograms represent all grayscale level values within region of interest (ROI). Dotted line, ROI. F, subcutaneous fat. M, muscle. B, bone. b. (i) EIM measures voltage after a current is applied. Diseased muscle has larger voltage and decreased phase shift. (ii) EIM is non-invasive. (iii) A difference between control and DMD phase data is shown.

Bony landmarks were used, when possible, to identify the muscle of interest. One rater measured the median GSL and QBA from each muscle image; two raters repeated 36 measurements from a representative sample of images for reliability analyses. Two examiners completed US biceps measurements in each subject for the purposes of interexaminer reliability; one examiner also completed two independent US biceps measurements for the determination of intraexaminer reliability. Electronic calipers were used to determine the SF thickness of each US image by measuring the distance from the dermis to the ventral fascia.

3.4 Quantitative Backscatter Analysis

Each ultrasound file was exported into a MATLAB® file using software provided by ultrasound manufacturer Terason®. Raw ultrasound data was mixed to baseband and then logarithmically converted to backscatter intensity values (measured in decibels, dB) using a MATLAB® program provided by Terason®. The median backscatter intensities of a superficial ROI placed on each ultrasound image was then calculated.

3.4 Data analysis

Mann-Whitney tests were performed to distinguish between DMD and healthy subjects, and the means and ranges were reported as (mean, range). Spearman correlations were performed to determine the relationships between GSL, EIM parameters, SF, age, and NSAA. A p-value of <0.05 was considered significant. Intraclass correlations, Bland-Altman analysis, and percent variation values were calculated to determine intra- and interrater as well as intra- and interexaminer reliability. Data was evaluated for individual muscles as well as with average values of the six muscles investigated.

3.5 Role of author

Development of the research area of focus was a collaborative effort at all stages by Irina Shklyar (IS) and PI Seward Rutkove (SR) based on an existing NIH grant authored by SR to study EIM and QUS in DMD subjects. Together, SR and IS determined that IS would focus on analyzing raw QBA data, in particular, of DMD patients. IS drafted the original research proposal with iterative feedback from SR. Subjects were recruited by research collaborators. IS collected EIM and US data, in collaboration with other researchers and research assistants. IS led the analysis of all data (except EIM reliability, which was completed by a

collaborator) and then planned and performed all XL Stat and MedCalc analyses; MATLAB® programming was provided by research collaborators, and US file conversion software was provided by the US manufacturer, Terason®. IS created the Figures, Tables, and manuscript with iterative feedback from SR.

4. RESULTS

4.1 Subject demographics

Twenty-five boys with DMD and twenty-five healthy boys were recruited. Of these, 14 DMD subjects underwent the NSAA. All boys were age 2 to 14 years with a mean age of 7.8 (2.2-13.4) years in DMD subjects and 7.7 (2.1-12.6) years in control subjects. Subject demographics are shown in Table 2. There was no significant differences between DMD and control subjects for age and weight, but DMD subjects were significantly shorter than their control counterparts (p=0.04). At the time of the study, 56% (14/25) of patients with DMD were on corticosteroids.

Table 2. Demographics for DMD and control patients. Data is expressed as mean (range). NS, not significant.

	DMD	Control	p value
Mean Age (Range) (yrs) (n=25 DMD, 25 control)	7.8 (2.2-13.4)	7.7 (2.1-12.6)	NS
Mean Weight (Range) (kg) (n=22 DMD, n=23 control)	27.2 (12.0-65.0)	27.6 (12.7-41.8)	NS
Mean Height (Range) (cm) (n=20 DMD, n=23 control)	117 (86-165)	129 (88-157)	0.04

[A.] Data is expressed as mean (range).
[B.] NS, not significant.

4.2 Identification of disease status

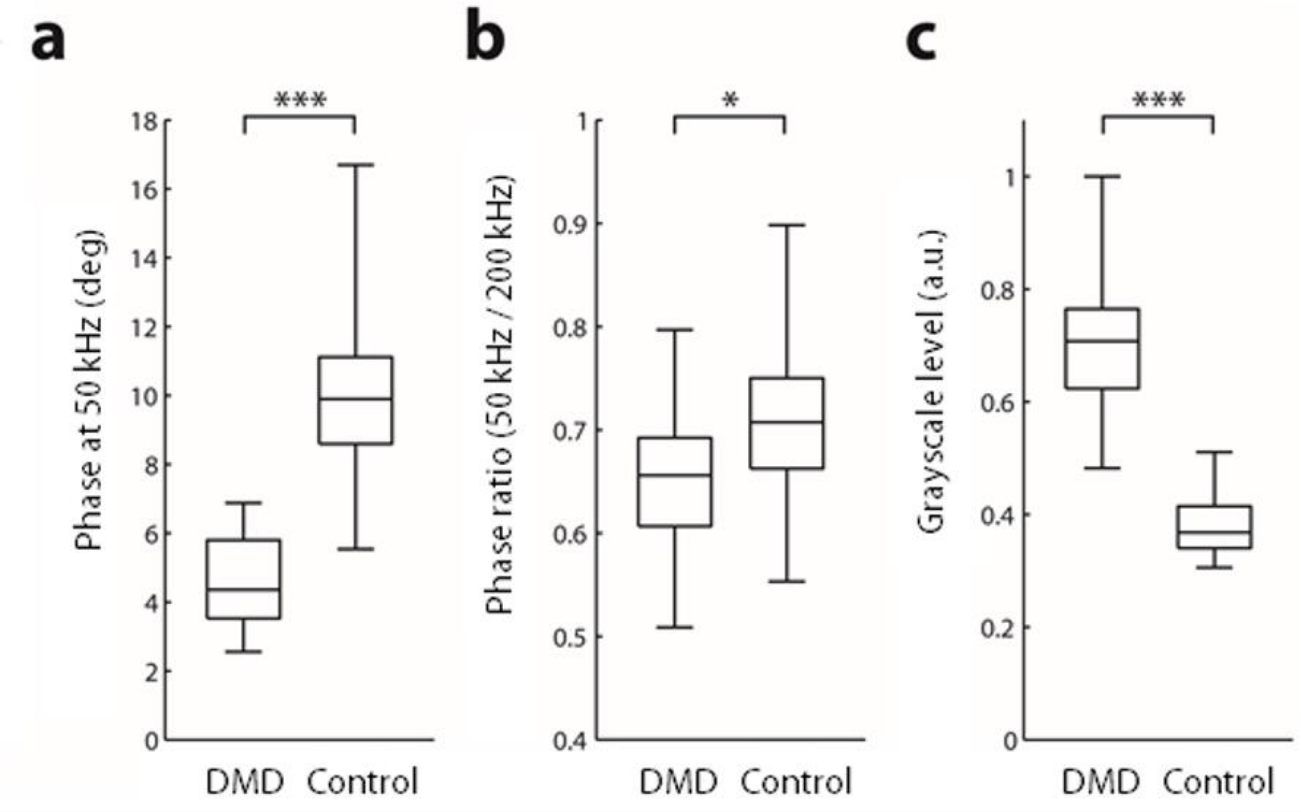

Figure 2. EIM and QUS measurements for six muscle average in DMD and control subjects. a. DMD subjects had significantly lower phase at 50 kHz values compared with controls (DMD: 4.26, 2.55-6.88; control: 9.86, 5.54-16.70, p<0.0001). **b.** Phase ratio (50 kHz / 200 kHz) values were significantly lower in DMD subjects (0.65, 0.51-0.71) than in controls (0.71, 0.55-0.90, p=0.018). **c.** Ultrasound grayscale level (GSL) measurements were also able to significantly (p<0.0001) distinguish between DMD (0.72, 0.48-1.00) and control subjects (0.38, 0.31-0.51). GSL values were scaled. Data expressed as (mean, range). a.u., arbitrary units. *p<0.05, **p<0.01, ***p<0.001.

The phase at 50 kHz and GSL demonstrated excellent differentiation between DMD patients and controls in all six muscles (p<0.0001). The phase ratio likewise demonstrated very good differentiation (p<0.02). The EIM 50 kHz phase

averaged across six muscles was significantly lower in dystrophic muscle (4.26, 2.55-6.88) than healthy muscle (9.86, 5.54-16.70) ($p<0.0001$). Phase ratio (50 kHz/200 kHz) values were significantly lower in DMD subjects (DMD: 0.65, 0.51-0.71) compared with controls (0.71, 0.55-0.90, $p=0.018$).

The averaged GSL measurements were significantly higher in DMD subjects (52.27, 38.67-66.17) than control subjects (28.06, 22.83-33.50) ($p<0.0001$), as shown in Figure 2.

4.3 Changes in EIM and GSL with Age

The 50 kHz phase decreased with age in DMD subjects in biceps (rho=0.48, $p=0.018$) and quadriceps muscles (rho=-0.47, $p=0.019$); the decrease in phase with age in other muscles and the average across all muscles did not reach significance (rho=-0.030 to -0.35, $p>0.084$). The phase at 50 kHz increased with age in control subjects in nearly all muscles (rho values=0.41-0.69, $p<0.044$), except quadriceps (rho=0.37, $p=0.068$). The six muscle average correlated strongly with age in controls (rho=0.61, $p=0.001$). The relationships between EIM values and age are shown in Figure 3.

The phase ratio (50 kHz/200 kHz) correlated strongly with age in controls in individual and averaged muscles (rho=0.66-0.93, $p<0.0005$), as shown in Figure

3. The ratio also correlated with age in DMD subjects in wrist flexors (rho=0.51, p=0.01), but they did not correlate in other muscles or averaged muscles (rho=-0.27 to 0.34, p>0.11).

GSL values did not change significantly with increasing age in either DMD subjects (rho values=-0.19 to 0.36, p>0.066) or controls (rho values=-0.245 to 0.322, p>0.116). Figure 3 shows that GSL detects disease pathology from an early age. In contrast, DMD and control subjects began with relatively similar EIM values and diverged with age. Additionally, both GSL and EIM show pathologic values, i.e, high GSL and low EIM values, at early ages followed by slight improvement for several years and then subsequent decline.

4.4 Changes in EIM and GSL compared with NSAA

The 50 kHz phase was strongly correlated with the NSAA in all muscles (rho values=0.55-0.83, p<0.045), except medial gastrocnemius (rho=0.52, p=0.060) and tibialis anterior (rho=0.46, p=0.097). The averaged phase was very strongly correlated with the NSAA (rho=0.74, p=0.004). The phase ratio (50 kHz/200 kHz) correlated with the NSAA in quadriceps (rho=0.64, p=0.015) but not in other

muscles (rho=-0.133 to 0.440, p>0.115). GSL values did not significantly correlate with NSAA in individual or averaged muscles (rho values=-0.44 to -0.041, p>0.115).

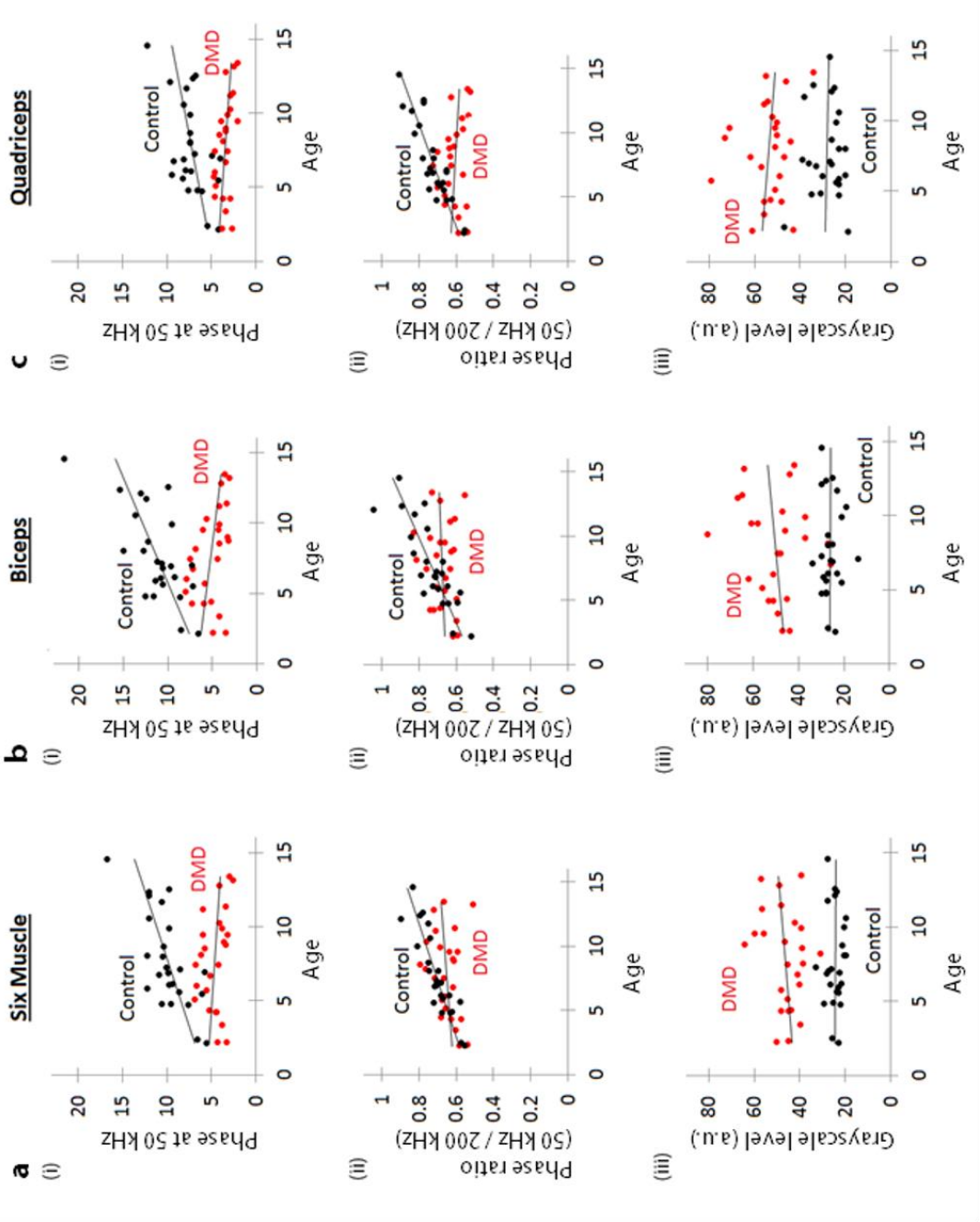

Figure 3. Scatter plots showing relationship between age and EIM and QUS parameters.

4.5 EIM and GSL analyses

The phase at 50 kHz correlated with GSL in dystrophic wrist flexors (rho=-0.40, p=0.048); the others muscles did not reach significance in DMD (rho=-0.29 to 0.26, p>0.071) or controls (rho=-0.27 to 0.0.33, p>0.10). We investigated a new phase ratio that has been optimized to eliminate the effect of subcutaneous fat on measurements (r=0.16, p=0.45) compared to the standard phase at 50 kHz (r=-0.72, p<0.0001) in averaged muscles (Figures 4 and 5).

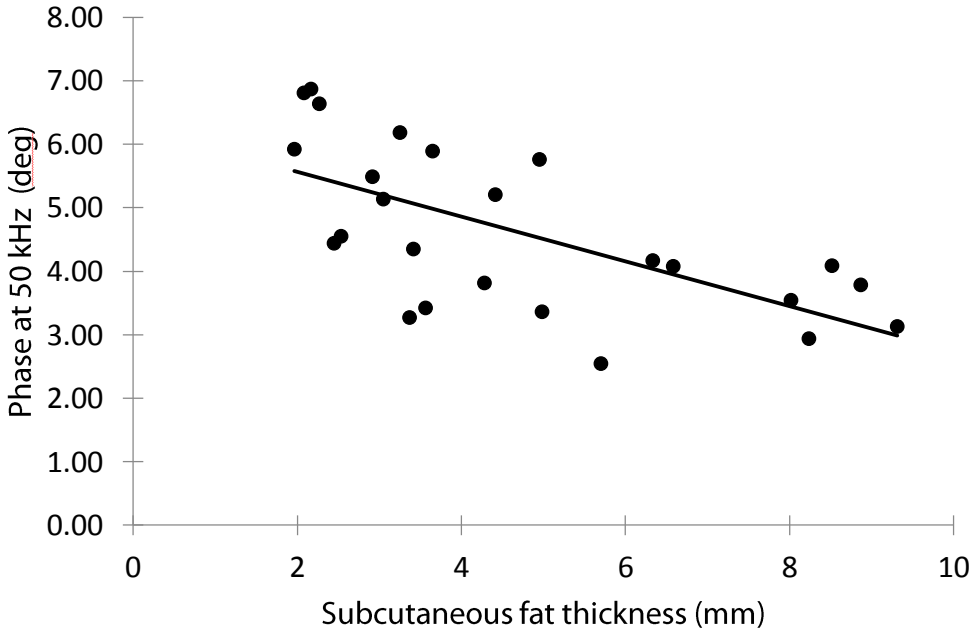

Figure 4. Scatter plot showing relationship between standard phase and subcutaneous fat for the average of six muscles. The phase at 50 kHz has a significant negative correlation with subcutaneous fat (rho=-0.72, p<0.0001).

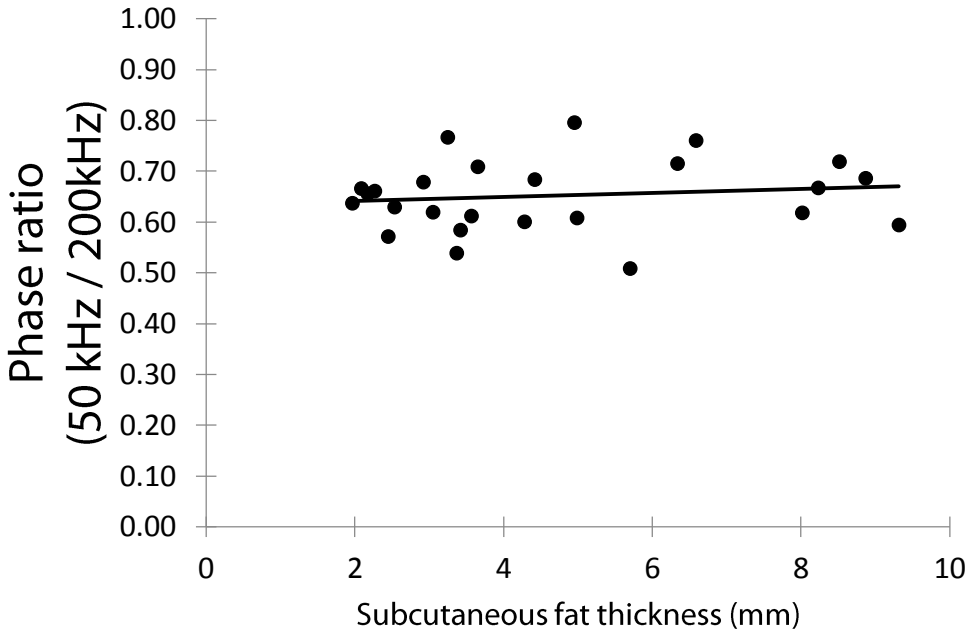

Figure 5. Scatter plot showing relationship between phase ratio and subcutaneous fat for the average of six muscles. Phase ratio (50 kHz / 200 kHz) has been optimized to eliminate the effect of subcutaneous fat on measurements (rho=0.16, p=0.45).

Table 3. Spearman correlations between EIM measurements and QUS measurements in DMD subjects are shown.

	50 kHz phase/GSL rho	Phase ratio/GSL rho
Deltoids	0.043	-0.20
Biceps	-0.055	-0.40*
Wrist Flexors	-0.40*	-0.0073
Quadriceps	0.26	0.15
Medial Gastrocnemius	-0.27	-0.40*
Tibialis Anterior	-0.29	-0.05
Six Muscle Average	-0.20	-0.48*

A. *p<0.05, **p<0.01, ***p<0.001.

The correlations between EIM parameters and GSL are shown in Table 3.

The phase ratio was inversely correlated with GSL in averaged muscles (rho=-0.48, p=0.017) as well as in biceps (rho=-0.40, p=0.046) and medial gastrocnemius (-0.040, p=0.046). It did not correlate with GSL in other muscles in DMD subjects (rho=-0.20 to 0.15, p>0.35) or controls (rho=-0.25 to 0.19, p>0.23), as shown in Figure 6.

4.6 Reliability analysis

Regarding ROI placement on US images, inter-rater (GSL: 0.99, QBA: 0.87) and intra-rater intraclass correlations (GSL: 0.96, QBA: 0.91) were excellent and comparable in GSL and QBA. Likewise, intra-examiner reliability with regard to ultrasound probe placement on biceps muscles (GSL ICC: 0.97, QBA ICC: 0.93) and inter-examiner reliability in biceps (GSL ICC: 0.94, QBA ICC: 0.91) are excellent when DMD and control subjects are combined, as seen in Table 4. Table 4 also shows the results of a Bland-Altman analysis, percent variation calculations, and intra- and inter-examiner variability with DMD and control subjects separated. The Bland-Altman plots are shown in Figures 7, 8, and 9, demonstrating acceptable coefficients of repeatability, bias away from the mean,

and degree of precision (values in Table 4). The distributions of repeated measures are also seen in Figures 7 and 8.

EIM was highly reliable in inter-session intra-examiner (all subjects: ICC 0.85-0.96, PV 8.31-16.86), inter-session inter-rater (ICC 0.90-0.94, PV 11.86-13.99), intra-session, inter-examiner (ICC 0.91-0.96, PV 8.95-11.61), and intra-session, intra-examiner (ICC: 0.95, PV 9.33) testing. Reliability for all subjects, DMD subjects, and control subjects are shown in Table 5.

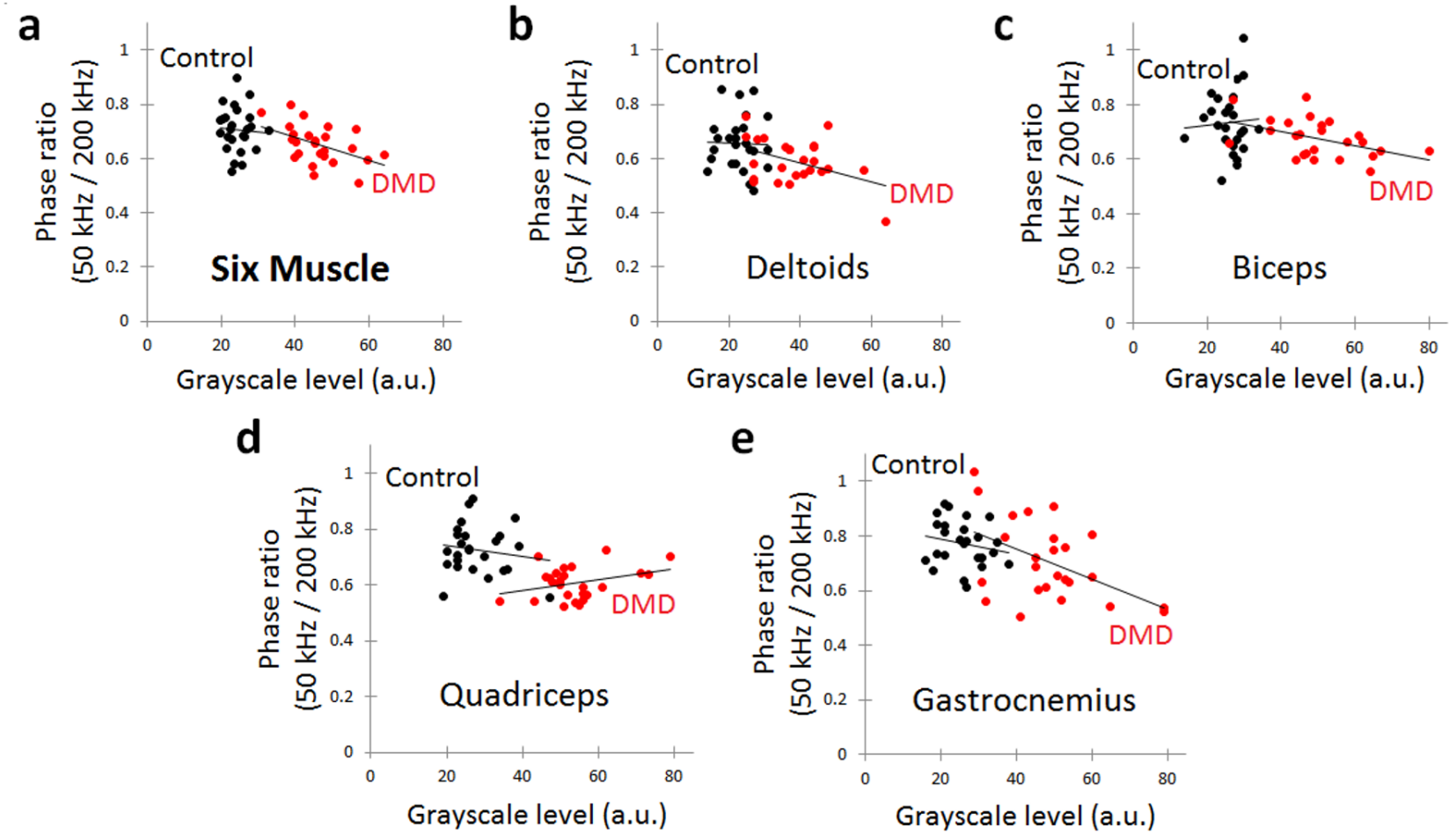

Figure 6. Scatter plots showing relationship between EIM measurements and QUS measurements in select muscles. a-e. EIM data are in the form of the ratio of phase at 50 kHz to phase at 200 kHz. QUS data was expressed as luminosity values (grayscale level, GSL). Six muscle, average of six muscles. a.u., arbitrary units.

Table 4. Intrarater, interrater, intraexaminer, and interexaminer reliability measurements comparing QUS and QBA.

	Bias	Precision	ICC	PV
Interrater GSL	1.07	8.91	0.99	4.86
Intrarater GSL	-6.71	13.76	0.96	8.67
Interrater QBA	8.02	8.39	0.87	8.11
Intrarater QBA	-7.26	6.67	0.91	6.10
Intraexaminer GSL Biceps DMD	-23.54	7.03	0.95	9.01
Intraexaminer GSL Biceps Control	1.83	14.44	0.52	19.86
Intraexaminer GSL Biceps Both	-8.04	9.57	0.97	14.66
Intraexaminer QBA Biceps DMD	2.74	2.98	0.93	4.38
Intraexaminer QBA Biceps Control	3.00	7.63	0.31	7.79
Intraexaminer QBA Biceps Both	7.04	4.20	0.93	6.16
Interexaminer GSL Biceps DMD	-0.44	12.66	0.86	14.26
Interexaminer GSL Biceps Control	11.48	15.89	0.42	21.85
Interexaminer GSL Biceps Both	4.86	14.22	0.94	18.21
Interexaminer QBA Biceps DMD	6.89	5.78	0.83	7.75
Interexaminer QBA Biceps Control	11.17	6.57	0.39	7.33
Interexaminer QBA Biceps Both	8.90	6.20	0.91	7.53
Interexaminer GSL Quads DMD	3.82	13.55	0.76	11.16
Interexaminer GSL Quads Control	-14.26	15.17	0.55	20.94
Interexaminer GSL Quads Both	-4.14	14.34	0.89	16.26
Interexaminer QBA Quads DMD	-31.55	11.97	-0.27	14.40
Interexaminer QBA Quads Control	-28.42	6.32	0.36	9.00
Interexaminer QBA Quads Both	-23.11	10.34	0.51	11.59

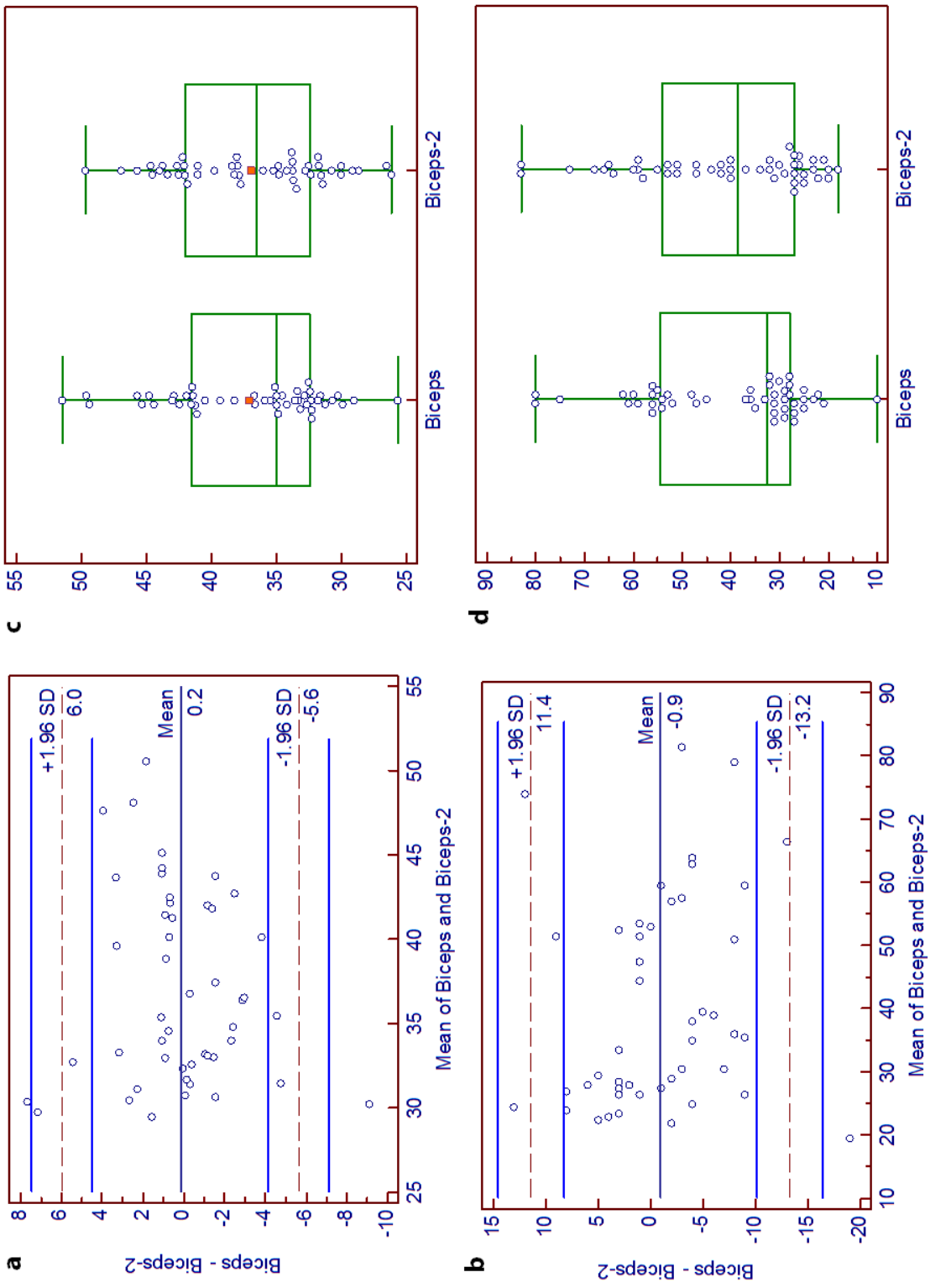

Figure 7. Comparison of QBA and GSL intraexaminer reliability in biceps brachii. . One examiner took two independent measurements of the biceps muscle in each subject. Biceps, examiner 1 first attempt. Biceps-2, examiner 1 second attempt. **a.** QBA Bland-Altman plot. **b.** GSL Bland-Altman plot. **c.** Distribution of QBA values. **d.** Distribution of GSL values.

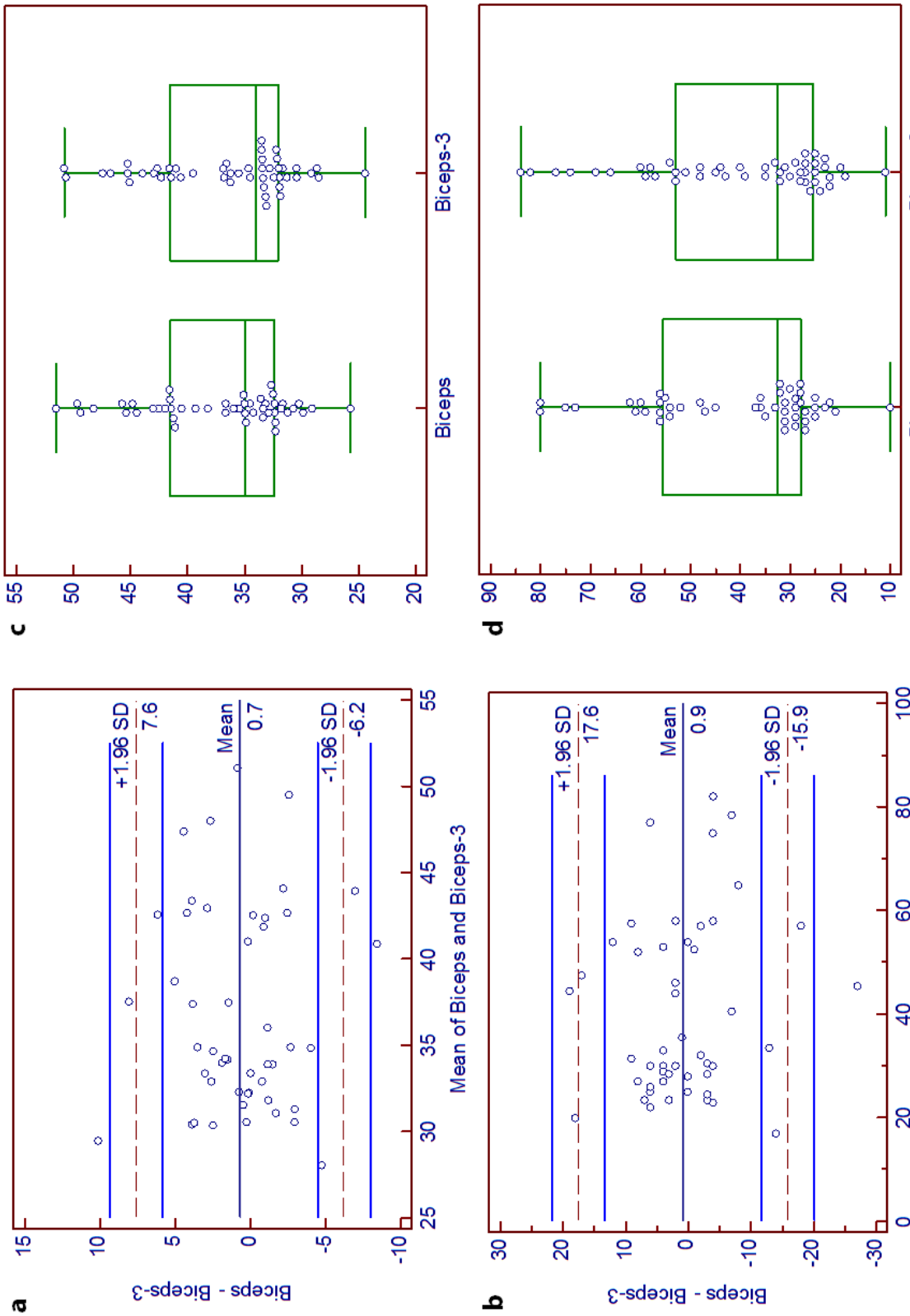

Figure 8. QBA and GSL Interexaminer reliability in biceps brachii. Two examiners took two independent measurements of the biceps muscle in each subject. Biceps, examiner 1. Biceps-3, examiner 2. **a.** QBA Bland-Altman plot. **b.** GSL Bland-Altman plot. **c.** Distribution of QBA values. **d.** Distribution of GSL values.

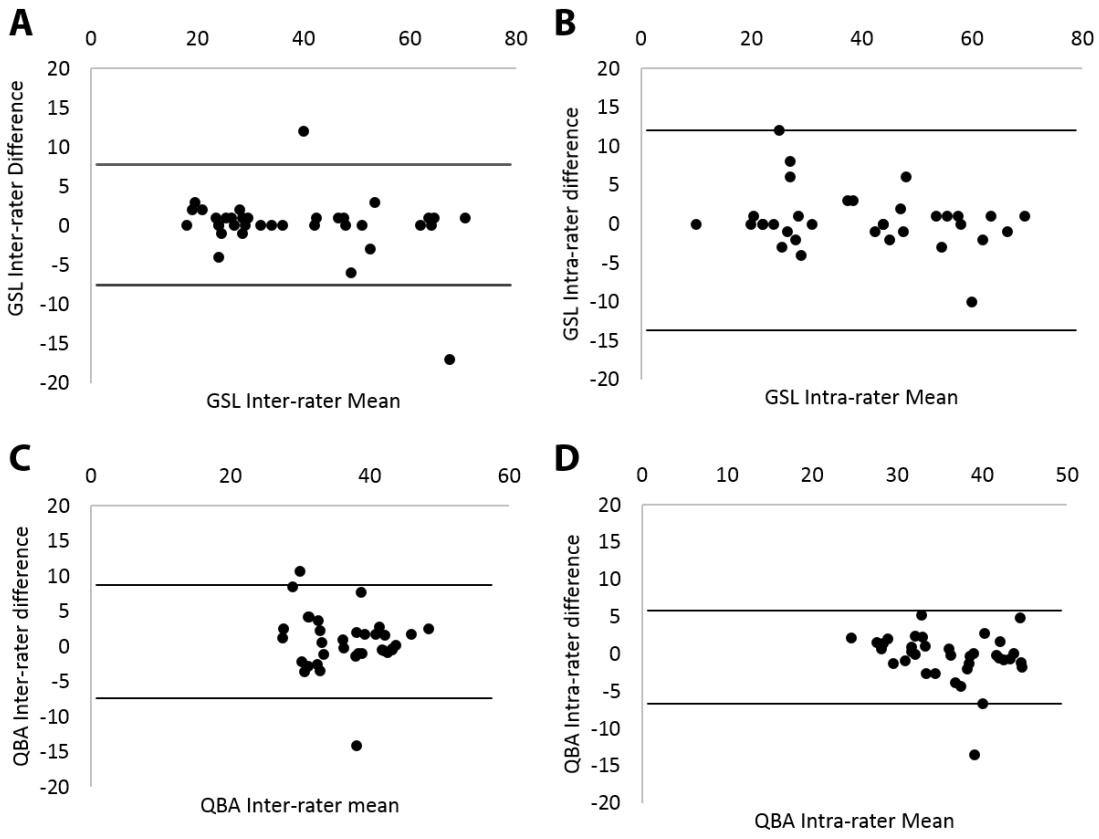

Figure 9. Intrarater and interrater Bland-Altman analysis.
Both grayscale (GSL, top panels) and quantitative backscatter (QBA, bottom panels) show good interrater (a and c) and intrarater (b and d) reliability. a. GSL interrater Bland-Altman plot with CR=5.23. b. GSL intrarrater Bland-Altman plot with CR=8.69. c. QBA interrater Bland-Altman plot with CR=5.78. d. QBA Intrarater Bland-Altman plot with CR=4.28. CR, coefficient of repeatability.

Table 5. Inter-session intra-examiner and inter-rater reliability as well as intra-session inter-examiner and intra-examiner reliability for electrical impedance myography (EIM).

INTER-SESSION MEASURES-INTRA-EXAMINER	ALL			DMD			Control		
Muscle/Group	ICC	Percent variation	N	ICC	Percent variation	N	ICC	Percent variation	N
Deltoid	0.94	11.91	33	0.90	16.98	13	0.88	8.61	20
Biceps	0.87	16.86	33	0.86	20.89	13	0.69	14.24	20
Forearm Flexors	0.96	11.30	33	0.83	18.24	13	0.94	6.79	20
Quadriceps	0.95	10.53	35	0.83	16.73	13	0.86	6.86	22
Tibialis Anterior	0.85	13.56	34	0.95	11.20	13	0.66	15.03	21
Medial Gastrocnemius	0.89	13.42	34	0.95	12.65	13	0.77	13.89	21
Six muscle average	0.96	8.31	29	0.97	8.57	12	0.90	8.14	17
INTER-SESSION MEASURES-INTER-RATER	**ALL**			**DMD**			**Control**		
Muscle/Group	ICC	Percent variation	N	ICC	Percent variation	N	ICC	Percent variation	N
Biceps	0.90	13.99	32	0.89	15.96	12	0.75	12.81	20
Quadriceps	0.94	13.46	33	0.82	20.67	12	0.84	9.34	21
Two-muscle average	0.94	11.86	31	0.89	16.46	12	0.82	8.95	19
INTRA-SESSION, INTER-EXAMINER MEASURES	**ALL**			**DMD**			**Control**		
Muscle/Group	ICC	Percent variation	N	ICC	Percent variation	N	ICC	Percent variation	N
Biceps	0.95	11.61	55	0.83	14.83	31	0.93	7.45	24
Quadriceps	0.91	11.31	56	0.83	11.07	30	0.78	11.59	26
Two-muscle average	0.96	8.95	53	0.88	9.65	30	0.92	8.03	23
INTRA-SESSION, INTRA-EXAMINER MEASURES	**ALL**			**DMD**			**Control**		
Muscle/Group	ICC	Percent variation	N	ICC	Percent variation	N	ICC	Percent variation	N
Biceps	0.95	9.33	56	0.94	9.10	31	0.89	9.61	25

Table 6. Comparison of QBA and GSL values in DMD and control subjects using Mann-Whitney tests.

GSL		Mean	Minimum	Maximum	p value	QBA		Mean	Minimum	Maximum	p value
Deltoid	DMD	45	31	68	< 0.0001	Deltoid	DMD	39	34	46	< 0.0001
	Control	26	21	34			Control	32	28	34	
Biceps	DMD	54	29	80	< 0.0001	Biceps	DMD	42	31	51	< 0.0001
	Control	28	10	36			Control	33	26	37	
Wrist Flexors	DMD	45	25	64	< 0.0001	Wrist Flexors	DMD	39	30	49	< 0.0001
	Control	20	8	29			Control	29	22	36	
Quadriceps	DMD	63	33	86	< 0.0001	Quadriceps	DMD	44	36	52	< 0.0001
	Control	35	22	53			Control	33	30	36	
Tibialis Ant	DMD	54	33	70	< 0.0001	Tibialis Ant	DMD	42	36	48	< 0.0001
	Control	29	18	39			Control	33	28	38	
Med Gastroc	DMD	55	31	77	< 0.0001	Med Gastroc	DMD	42	33	50	< 0.0001
	Control	30	22	45			Control	34	30	40	
Six Muscle	DMD	53	38	67	< 0.0001	Six Muscle	DMD	41	36	47	< 0.0001
	Control	28	23	34			Control	33	30	36	

4.7 QBA analysis

QBA and GSL from all muscles were higher in DMD subjects than controls ($p<0.001$). In the six muscle average of GSL values, for example, dystrophic muscle (53, 38-67) is significantly brighter than healthy muscle (28, 23-34), as shown in Table 6 ($p<0.0001$). This is also the case in averaged QBA values in DMD subjects (41, 36-47) and control subjects (33, 30-36; $p<0.0001$).

Average QBA correlated highly with average GSL in DMD (rho =0.90, $p<0.0001$). The correlations between individual muscles are shown in Figure 10.

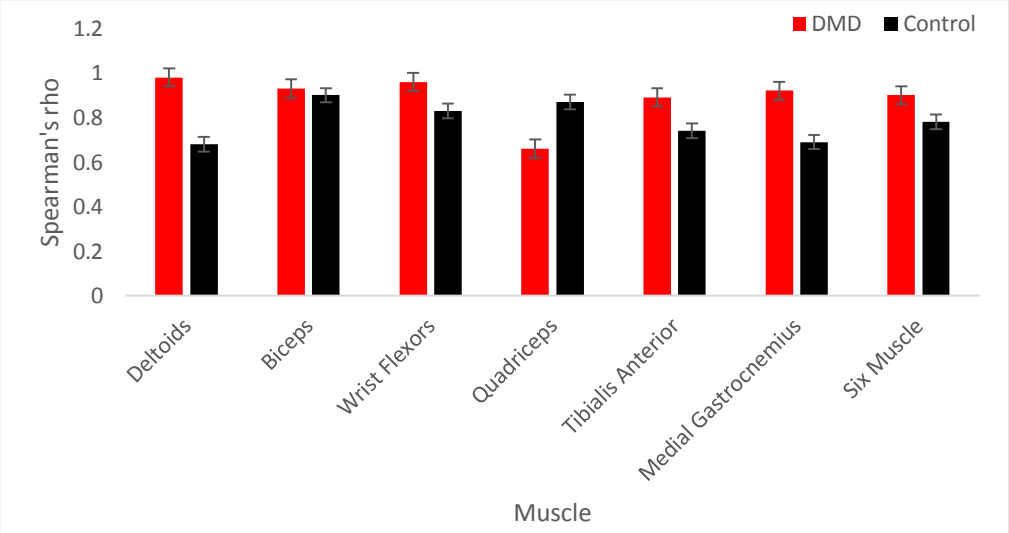

Figure 10. Spearman correlations between QBA and GSL in DMD and control subjects. Correlations were higher in DMD subjects compared with controls in most muscles. QBA and GSL DMD quadriceps values did not correlate strongly.

In DMD, both GSL and QBA increased with age more substantially in upper than lower extremity muscles (Table 7). Correlations with age and GSL or QBA were strongest in the deltoid and absent in the quadriceps and medial gastrocnemius. The tibialis anterior and average muscle GSL and QBA increased with worse performance on the NSAA. Correlations to either age or NSAA were similar ($p \geq 0.16$) between GSL and QBA. In controls, neither GSL nor QBA varied with age ($rho < 0.17$, $p > 0.13$).

Correlations between the QUS parameters and NSAA were evident in tibialis anterior with both parameters and in averaged muscles when correlated with GSL (Table 8).

Table 7. Spearman correlations between ultrasound parameters and age.

		Deltoids	Biceps	Wrist Flexors	Quadriceps	Tibialis Anterior	Medial Gastrocnemius	Six Muscle
DMD GSL	Spearman's rho	0.63	0.38	0.53	0.20	0.40	0.058	0.47
	p value	0.001	0.061	0.008	0.34	0.05	0.78	0.020
Control GSL	Spearman's rho	0.030	0.050	-0.32	0.059	0.15	-0.20	-0.085
	p value	0.89	0.81	0.13	0.78	0.48	0.33	0.69
DMD QBA	Spearman's rho	0.7	0.54	0.58	0.014	0.45	0.11	0.67
	p value	0.0002	0.006	0.003	0.95	0.02	0.6	0.0004
Control QBA	Spearman's rho	0.097	0.17	-0.20	0.003	0.14	-0.11	-0.002
	p value	0.64	0.43	0.33	0.99	0.50	0.61	0.99

Table 8. US parameter and NSAA Spearman correlations in DMD subjects.

GSL		rho	p value
	Deltoids	-0.33	0.25
	Biceps	-0.28	0.34
	Wrist Flexors	-0.18	0.54
	Quadriceps	-0.17	0.56
	Tibialis Anterior	-0.68	0.009
	Medial Gastrocnemius	-0.44	0.12
	Six Muscle	-0.60	0.03
QBA		rho	p value
	Deltoids	-0.36	0.21
	Biceps	-0.20	0.50
	Wrist Flexors	-0.19	0.52
	Quadriceps	-0.31	0.28
	Tibialis Anterior	-0.76	0.003
	Medial Gastrocnemius	-0.27	0.35
	Six Muscle	-0.59	0.03

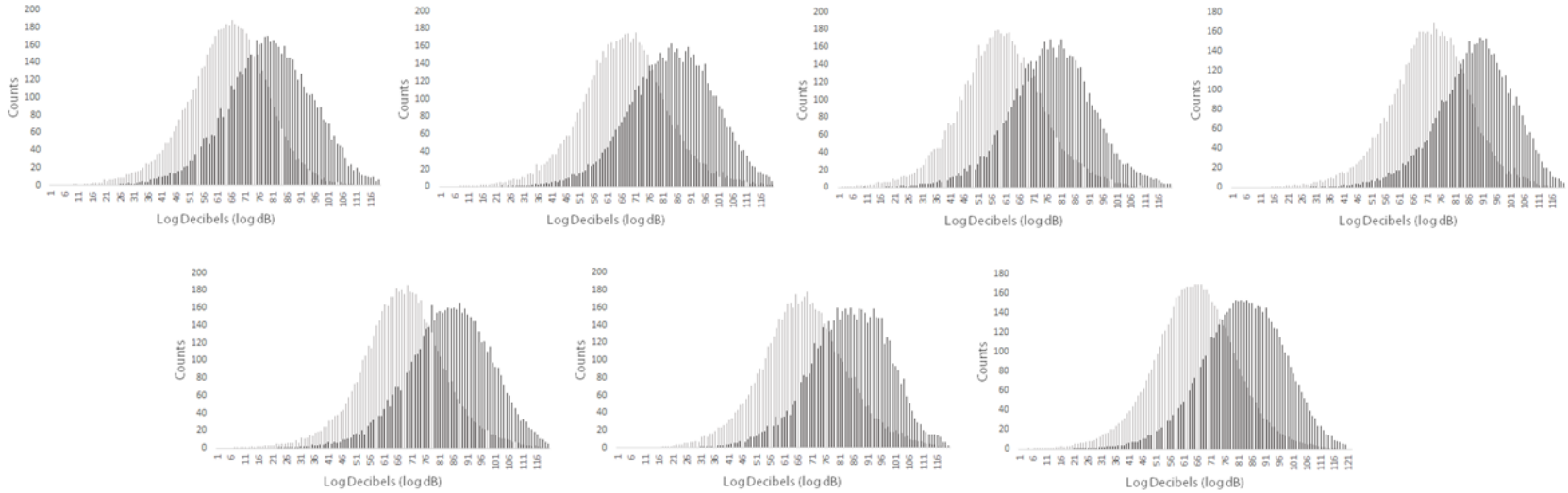

Figure 11. Histograms representing raw backscatter values in log decibels (log dB). Dark gray: DMD. Light gray: control. Backscatter values demonstrate a right shift compared with control values. a) Deltoids. b) Biceps. c) Wrist flexors. d) Quadriceps. e) Tibialis anterior. f) Medial gastrocnemius. g) Six muscle average.

5. DISCUSSION

5.1 Summary of EIM and QUS analysis

EIM and QUS show promise as new biomarkers for DMD clinical trials. These quantitative technologies are painless, sensitive, and non-invasive surrogate measures of disease progression that may aid the rapid identification of successful therapeutics currently in clinical pipelines. The EIM and QUS parameters demonstrated excellent separation between DMD and control subjects. We used age and NSAA as surrogates for disease severity. The NSAA correlated very strongly with the 50 kHz phase in four of six muscles, but it did not correlate with GSL of the entire muscle (whole muscle GSL) or phase ratio.

The 50 kHz phase significantly increased with age in controls, except for quadriceps, and declined in the measurements of biceps and quadriceps of DMD subjects. The correlation with age in healthy muscle suggests that EIM identifies characteristics of normal growth that are lost in DMD. The absence of a significant correlation between phase and age in other dystrophic muscles appears to reflect the "honeymoon period" wherein DMD subjects improve before they decline [27]. Therefore, there is a non-linear relationship between the parameters and age, resulting in a non-significant correlation.

Whole muscle GSL values reveal a large difference between DMD and control subjects at an early age, and that difference remains stable across all ages. In contrast, EIM values of DMD and control subjects become increasingly disparate with age. This may indicate that GSL values would make good biomarkers in early stages of disease, while EIM may prove more useful in advanced stages.

Additionally, EIM is highly reliable with ICC values above 0.85 in inter-examiner and intra-examiner testing within and between sessions.

5.2 A new EIM parameter: phase ratio

A new EIM parameter, the phase ratio (50 kHz / 200 kHz), nearly eliminates the confounding effect of subcutaneous fat compared with the phase at 50 kHz in standard use. The phase ratio has a stronger correlation with GSL than phase at 50 kHz in DMD subjects. This suggests that the phase ratio and GSL share more information about diseased muscle than the phase at 50 kHz with GSL due to the elimination of the effect of subcutaneous fat.

5.3 EIM and QUS correlations

The reason the correlations between the EIM and QUS look strong in some muscles, such as biceps and medial gastrocnemius, and poor in others, such as quadriceps, may be that the quadriceps change at an earlier age and level off

more quickly. In contrast, biceps muscles appear to change slowly with age, resulting in a stronger linear correlation between the parameters and age.

5.4 Superficial versus whole muscle regions of interest

GSL showed stronger correlations with age using the superficial ROI compared with the whole muscle ROI, likely due to the absence of image attenuation with the smaller superficial ROI. This is consistent with prior work wherein the upper one-third of a drawn polygon was used to obtain GSL values [28].

5.5 A new approach to quantitative ultrasound in DMD: quantitative backscatter analysis

Both QBA and GSL show high intra- and interrater as well as well as intra- and interexaminer reliability. Both QBA and GSL are able to distinguish dystrophic muscle from healthy muscle due to the higher echogenicity in the former. As might be expected, QBA and GSL correlate strongly with each other in DMD subjects. These correlations are not as strong in control subjects because

all controls have low GSL and QBA values; there is no dynamic range that would result in a strong correlation in control subjects.

NSAA correlations with QUS parameters were inconsistent across muscles. Tibialis anterior was the only individual muscle to demonstrate a correlation in both parameters; this is consistent with the whole muscle ROI correlations with NSAA, which likewise did not demonstrate strong correlations with NSAA.

The information present in QBA is comparable to that seen in GSL; thus, post-processing of raw ultrasound frequency data does not result in falsely positive findings. GSL demonstrated a linear relationship with QBA, demonstrating comparable information across a broad range of values. Furthermore, QBA avoids differences in post-processing across ultrasound manufacturers, rendering it easy to implement in multicenter trials with diverse manufacturers. In addition, QBA is measured in decibels while GSL is dimensionless.

5.6 Limitations and future directions

Limitations of this work include the relatively small sample size as well as the use of three sizes of handheld EIM array, depending on the size of the children, since this may introduce additional variability. Additionally, further study is needed of reactance and resistance EIM data, EIM and QUS data in younger

versus older subjects to reflect the non-linear data, and longitudinal EIM data with the probe parallel to the muscle fibers. Additionally, multi-year data collection is in progress to compare EIM and QUS parameters as measures of disease progression to functional measures currently in use.

The moderate correlation between phase at 50 kHz and GSL in averaged muscles indicate that there is overlapping information about diseased muscle; however the absence of a complete linear correlation indicate that the measures may provide acoustic and electrical information that supplement one another. Prior work has explored the use of a machine-learning algorithm to create a composite EIM-QUS biomarkers in spinal muscle atrophy (SMA) [29]. Therefore, future work will explore the possibility of an EIM-QUS composite outcome measure uniquely suited to DMD.

Acknowledgments: This work was funded by the NIH (R01AR060850-02). IS was funded by the Howard Hughes Medical Institute (HHMI) and Duchenne Research Fund (DRF).

REFERENCES

1. Bushby K, Finkel R, Birnkrant DJ, et al. Diagnosis and management of Duchenne muscular dystrophy, part 1: diagnosis, and pharmacological and psychosocial management. Lancet Neurol 2010;9:77-93.
2. Manzur AY, Kuntzer T, Pike M, Swan A. Glucocorticoid corticosteroids for Duchenne muscular dystrophy. Cochrane Database Syst Rev 2008:CD003725.
3. Enright PL. The six-minute walk test. Respir Care 2003;48:783-5.
4. Mazzone, E. S., Messina, S., Vasco, G., Main, M., Eagle, M., D'Amico, A., ... & Mercuri, E. (2009). Reliability of the North Star Ambulatory Assessment in a multicentric setting. *Neuromuscular Disorders*, *19*(7), 458-461.
5. Bushby K, Edward C. Clinical outcome measures for trials in Duchenne muscular dystrophy: report from International Working Group meetings. Clinical Investigation 2011; 1(9):1217.
6. Finkel R, Wong B, Bushby A, et al. Results of a Phase 2b, dose-ranging study of ataluren (PTC124®) in nonsense mutation Duchenne/Becker muscular dystrophy (nmDBMD). Neuromuscular Disorders 2010; 20(9-

10): 656-7.

7. Prior TW, Bridgeman SJ. Experience and strategy for the molecular testing of Duchenne muscular dystrophy. J Mol Diagn 2005;7:317-26.

8. Wren TA, Bluml S, Tseng-Ong L, Gilsanz V. Three-point technique of fat quantification of muscle tissue as a marker of disease progression in Duchenne muscular dystrophy: preliminary study. AJR Am J Roentgenol 2008;190:W8-12.

9. Pillen S, Arts IM, Zwarts MJ. Muscle ultrasound in neuromuscular disorders. Muscle Nerve 2008;37:679-93.

10. Pillen S, Tak RO, Zwarts MJ, et al. Skeletal muscle ultrasound: correlation between fibrous tissue and echo intensity. Ultrasound Med Biol 2009;35:443-6.

11. Wu JS, Darras BT, Rutkove SB. Assessing spinal muscular atrophy with quantitative ultrasound. Neurology 2010;75:526-31.

12. Zaidman CM, Connolly AM, Malkus EC, Florence JM, Pestronk A. Quantitative ultrasound using backscatter analysis in Duchenne and Becker muscular dystrophy. Neuromuscul Disord 2010;20:805-9.

13. Nair A, Kuban BD, Obuchowski N, Vince DG. Assessing spectral algorithms to predict atherosclerotic plaque composition with normalized and raw intravascular ultrasound data. Ultrasound Med

Biol 2001;27:1319-31.

14. Zaidman CM, Holland MR, Anderson CC, Pestronk A. Calibrated Quantitative Ultrasound Imaging of Skeletal Muscle Using Backscatter Analysis. Muscle & Nerve 2008; 38: 893-8.

15. Aaron R, Esper GJ, Shiffman CA, Bradonjic K, Lee KS, Rutkove SB. Effects of age on muscle as measured by electrical impedance myography. Physiol Meas 2006;27:953-9.

16. Ahad MA, Rutkove SB. Finite element analysis of electrical impedance myography in the rat hind limb. Conf Proc IEEE Eng Med Biol Soc 2009;2009:630-3.

17. Esper GJ, Shiffman CA, Aaron R, Lee KS, Rutkove SB. Assessing neuromuscular disease with multifrequency electrical impedance myography. Muscle Nerve 2006;34:595-602.

18. Garmirian LP, Chin AB, Rutkove SB. Discriminating neurogenic from myopathic disease via measurement of muscle anisotropy. Muscle Nerve 2009;39:16-24.

19. Rutkove SB, Esper GJ, Lee KS, Aaron R, Shiffman CA. Electrical impedance myography in the detection of radiculopathy. Muscle Nerve 2005;32:335-41.

20. Rutkove SB, Zhang H, Schoenfeld DA, et al. Electrical impedance myography to assess outcome in amyotrophic lateral sclerosis clinical trials. Clin Neurophysiol 2007;118:2413-8.

21. Shiffman CA, Aaron R, Rutkove SB. Electrical impedance of muscle during isometric contraction. Physiol Meas 2003;24:213-34.

22. Tarulli A, Esper GJ, Lee KS, Aaron R, Shiffman CA, Rutkove SB. Electrical impedance myography in the bedside assessment of inflammatory myopathy. Neurology 2005;65:451-2.

23. Tarulli AW, Duggal N, Esper GJ, et al. Electrical impedance myography in the assessment of disuse atrophy. Arch Phys Med Rehabil 2009;90:1806-10.

24. Tarulli AW, Garmirian LP, Fogerson PM, Rutkove SB. Localized muscle impedance abnormalities in amyotrophic lateral sclerosis. J Clin Neuromuscul Dis 2009;10:90-6.

25. Rutkove, S. B., Shefner, J. M., Gregas, M., Butler, H., Caracciolo, J., Lin, C., ... & Darras, B. T. (2010). Characterizing spinal muscular atrophy with electrical impedance myography. *Muscle & nerve*, *42*(6), 915-921.

26. Narayanaswami, P., Spieker, A. J., Mongiovi, P., Keel, J. C., Muzin, S. C., & Rutkove, S. B. (2012). Utilizing a handheld electrode array for

localized muscle impedance measurements. *Muscle & nerve*, *46*(2), 257-263.

27. Li, J., Geisbush, T. R., Rosen, G. D., Lachey, J., Mulivor, A., & Rutkove, S. B. (2013). Electrical impedance myography for the in and ex vivo assessment of muscular dystrophy (mdx) mouse muscle. *Muscle & Nerve*.

28. Escolar, D. M., Buyse, G., Henricson, E., Leshner, R., Florence, J., Mayhew, J., ... & Wessel, H. (2005). CINRG randomized controlled trial of creatine and glutamine in Duchenne muscular dystrophy. *Annals of neurology*, *58*(1), 151-155.

29. Jansen, M., van Alfen, N., Nijhuis van der Sanden, M. W., van Dijk, J. P., Pillen, S., & de Groot, I. J. (2012). Quantitative muscle ultrasound is a promising longitudinal follow-up tool in Duchenne muscular dystrophy. *Neuromuscular Disorders*, *22*(4), 306-317.

30. Srivastava, T., Darras, B. T., Wu, J. S., & Rutkove, S. B. (2012). Machine learning algorithms to classify spinal muscular atrophy subtypes. *Neurology*, *79*(4), 358-364.